Journal of Dental Sciences 19 (2024) 1506–1514

Available online at www.sciencedirect.com

ScienceDirect

journal homepage: www.e-jds.com

Original Article

Involvement of miR-199a-5p-loaded mesoporous silica nanoparticle-polyethyleneimine-KALA in osteogenic differentiation

Tianyue Wang [a,b*], Hidemi Nakata [a,b**], Bing Shen [e], Ziying Jiao [e], Kaori Yokota [a,b], Shinji Kuroda [a,b,c], Shohei Kasugai [a,b,d], Eriko Marukawa [b]

[a] *Department of Oral Implantology and Regenerative Dental Medicine, Graduate School of Medical and Dental Sciences, Tokyo Medical and Dental University, Tokyo, Japan*
[b] *Department of Regenerative and Reconstructive Dental Medicine, Graduate School of Medical and Dental Sciences, Tokyo Medical and Dental University, Tokyo, Japan*
[c] *Improvement of Gnatho-oral Function, Department of Stomatognathic, Faculty of Dental Medicine, Hokkaido University, Hokkaido, Japan*
[d] *Dental Clinic, Southern TOHOKU General Hospital, Fukushima, Japan*
[e] *Department of Physiology, School of Basic Medical Science, Anhui Medical University, Hefei, China*

Received 24 December 2023; Final revision received 8 January 2024
Available online 5 February 2024

KEYWORDS
MiR-199a-5p;
Micro RNA;
Mesoporous silica nanoparticles;
Nanodentistry;
Osteogenic differentiation

Abstract *Background/purpose:* While there are numerous reports on surgical techniques and materials for bone grafting, limited methods are available to enhance the body's inherent capacity to heal bones. Here we investigated microRNA-199a (miR-199a), a molecular that promotes osteoblast differentiation and bone healing.
Materials and methods: To construct a miR-199a delivery complex, miR-199a-5p mimics were coated with mesoporous silica nanoparticles (MSNs) following modified with polyethyleneimine (PEI) and peptide WEAKLAKALAKALAKHLAKALAKALKACEA (KALA) to obtain 199a-5p-loaded MSN-PEI-KALA. Nanoparticle complexes are assessed for particle size and zeta potential using transmission electron microscopy and dynamic light scattering. Then MC3T3-E1 cells are exposed to MSN_miR-199a-5p @PEI-KALA. The impact of MSN_miR-199a-5p@PEI-KALA at varying concentrations on cell viability is assessed using Cell Counting Kit-8. Cell uptake and distribution were analyzed by double fluorescent staining with fluorescein amidite-labeled

* Corresponding author. Department of Regenerative and Reconstructive Dental Medicine, Graduate School of Medical and Dental Sciences, Tokyo Medical and Dental University, 1-5-45 Yushima, Bunkyo-ku, Tokyo 113-8510, Japan.
** Corresponding author. Department of Regenerative and Reconstructive Dental Medicine, Graduate School of Medical and Dental Sciences, Tokyo Medical and Dental University, 1-5-45 Yushima, Bunkyo-ku, Tokyo 113-8510, Japan.
E-mail addresses: wtiairm@tmd.ac.jp (T. Wang), hidemi.irm@tmd.ac.jp (H. Nakata).

https://doi.org/10.1016/j.jds.2024.01.007

MSN_miR-199a@PEI-KALA and lysosome labeling. On day 7 after osteogenic induction, alkaline phosphatase (ALP) staining was conducted.
Results: The findings indicated that the nanoparticle complexes encapsulating PEI and peptide exhibited an augmentation in both particle size and zeta potential. At a dosage of 10 μg/mL, MSN_miR-199a@PEI-KALA displayed the lowest cytotoxicity compared to the control group. MC3T3-E1 cells treated with MSN_miR-199a-5p@PEI-KALA exhibited intensified ALP staining and elevated mRNA expression levels of ALP, runt-related transcription factor 2, and osteopontin, suggesting the involvement of miR-199a-5p-loaded MSN-PEI-KALA in osteogenic differentiation.
Conclusion: The successful construction of the delivering complex MSN_miR-199a@PEI-KALA in present research highlights the promise of this biomaterial carrier for the application of miRNAs in treating bone defects.

Introduction

Nanodentistry is an extension of nanotechnology in dentistry that has revolutionized every branch of the field.[1] Nanomaterials are now used as therapeutic and diagnostic tools as well as aids in maintaining oral hygiene.[2] A comprehensive evaluation of the anatomy and physiology of the target site is essential for the advancement of biocompatible nanoproducts.[3] Despite the many limitations of revolutionary nanotechnology in terms of clinical applications, it has added a new dynamic to traditional dental techniques.[4]

Synthetic nanoparticles present a promising avenue for delivering plasmid DNA, various RNA types, and drugs.[5–8] Recently, there's a burgeoning interest in studying the biomedical potentials of mesoporous silica nanoparticles (MSNs).[5,9] MSNs boast a remarkable surface area of up to 1500 m^2/g and significant pore volumes reaching approximately 1 cm^3/g, enabling the retention of significant drug quantities owing to their textural properties.[10,11] These nanoparticles demonstrate excellent biocompatibility, biodegradability, adjustable physicochemical attributes, site-specific functionalization, and a robust framework.[8,12,13]

Furthermore, the Polyethyleneimine (PEI)-coated MSNs exhibit notable affinity for genes in the form of DNA, small interfering RNA (siRNA), and microRNA (miRNA).[14] However, PEI's high toxicity hinders clinical translation.[15] The WEAKLAKALAKALAKHLAKALAKALKACEA (KALA) peptides can condense nucleic acid drugs into multimers through electrostatic force, generally demonstrating significantly lower toxicity compared to traditional cationic polymers like PEIs.[16] Moreover, studies have demonstrated that KALA is capable of traversing the lipophilic cellular membrane barrier and deliver various reagents.[17–19] Recent research indicates that core-cone MSNs coated with PEI have the ability to promote bone regeneration by manipulating the microenvironment through both the nanoparticles and their carrier miRNA-26a.[20] The application of surface-modified MSNs promotes the development of bone marrow mesenchymal stromal cells by facilitating the transport of miRNA-26a.[21]

Numerous physiological and pathological processes are regulated by the miR-199 family. Among them, miR-199a-5p is a crucial molecule for the maintenance of bone homeostasis.[22,23] Its presence has also been observed in various cancer types, including colorectal and liver cancers.[24,25] Despite the growing attention in miRNA research, there are few articles on miR-199-loaded MSN. Hence, this study aims to investigate miR-199-based therapy for osteogenesis. A new delivery complex for miR-199a was created using MSNs coated with PEI and KALA, according to their characteristics.

Materials and methods

Construction of nanoparticles

The MSN_miR-199a@PEI-KALA was synthesized by modifying previously reported methods.[21] Initially, 1 mg MSN (Jiancheng Bioengineering, Nanjing, China), 160 μL ethanol (Sigma-Aldrich, St. Louis, MO, USA), and 40 μL 4M Guanidine hydrochloride (MW = 95.53; Sigma-Aldrich) were mixed and subjected to ultrasonic treatment (P = 80 W) for 10 min. Following this, 20 μL of 0.1 nmol/μL miR-199a mimic or fluorescein amidite (FAM)-labeled miR-199a mimic or mimic NC (Sangon Biotech, Shanghai, China) or RNase-free water was added, and the mixture underwent sonication. At 4 °C, the mixture was shaken for 1 h at 200 rpm and subsequently underwent centrifugation at 12000 rpm for 10 min at the same temperature. After discarding the supernatant, the particles were sonicated with 400 μL of ethanol, and then 400 μL 1 mg/mL PEI (MW = 25,000Da; Sigma-Aldrich) ethanol solution was gradually added. After ultrasonic dispersion for another 15 min, the mixture underwent centrifugation, and the obtained particles—MSN coated with PEI (MSN@PEI), MSN_miR-NC@PEI, MSN_miR-199a@PEI were collected. Particles generated were resuspended in 400 μL ethanol, to which 40 μL of 0.2 mg/mL N-succinimidyl-3-(2-pyridyldithiol) propionate (SPDP; Sigma-Aldrich) was added. This mixture underwent a 15-min sonication, left to stand for 30 min, followed by centrifugation and discarding the supernatant. The sediment was sonicated in 400 μL RNase-free water, and 150 μL of 1 mg/mL KALA (Sangon Biotech) peptide was added. After another round of

sonication, it was left to stand for 30 min, centrifuged, and the supernatant discarded, resulting in the isolation of MSN@PEI-KALA, MSN_miR-NC@PEI-KALA, MSN_miR-199a@PEI-KALA. The particles were resuspended in RNase-free water and kept for future use at −20 °C (Fig. 1).

Characterization of nanoparticles

The morphology of MSN, MSN@PEI-KALA, MSN_miR-NC@PEI-KALA, MSN_miR-199a@PEI-KALA were observed with transmission electron microscopy (TEM; Talos L120C; Thermo Fisher Scientific, Waltham, MA, USA). The size and zeta potential of the nanoparticles in liquid solution were determined using dynamic light scattering (DLS; ZetaSizer Lab; Malvern Panalytical, Malvern, UK).

Cell culture

The MC3T3-E1 cells (iCell Bioscience, Shanghai, China) were cultured in Eagle's Minimum Essential Medium (MEM; Gibco™ Thermo Fisher Scientific, Warsaw, Poland) supplemented with 10 % Fetal Bovine Serum (FBS; Sigma-Aldrich) and 1 % Penicillin-Streptomycin (Sigma-Aldrich) in incubator under constant conditions. The medium was switched to osteogenic differentiation medium after incubation for 24 h. The osteogenic differentiation medium consisted of MEM with FBS, Penicillin-Streptomycin, ascorbic acid, sodium β-glycerophosphate, and dexamethasone (Sigma-Aldrich).

Cell viability assay

Cell Counting Kit-8 (CCK-8; Abbkine, Wuhan, China) was used to measure the cell viability in compliance with the manufacturer's instructions. Following seeding into 96-well plates, MC3T3-E1 cells were exposed to various doses (5, 10, 20, 40, and 60 μg/mL) of MSN@PEI-KALA, MSN_miR-NC@PEI-KALA and MSN_miR-199a@PEI-KALA. The control group consisted of the cells that were not given any treatment. Each well received 10 μL of CCK-8 after 48 h, and the mixture was incubated for 90 min at 37 °C. The microplate reader was used to test the samples' absorbance at 450 nm (Rayto, Shenzhen, China).

Fluorescent staining

The MC3T3-E1 cells were treated with 10 μg/mL FAM-labelled MSN_miR-199a@PEI-KALA. After 6 h of incubation, the medium was changed to Lyso-Tracker Red probe-containing medium (Solarbio, Beijing, China) for lysosome labelling. 4′,6-diamidino-2-phenylindole (4′,6-DAPI; Thermo Fisher Scientific) was used to mark the nuclei. Fluorescence microscopy was used to collect the fluorescent images. (DP73; Olympus, Tokyo, Japan).

Alkaline phosphatase staining

The MC3T3-E1 cells were treated with 10 μg/mL MSN@PEI-KALA, MSN_miR-NC@PEI-KALA, and MSN_miR-199a@PEI-KALA. The Alkaline Phosphatase (ALP) Staining Kit (Beyotime, Shanghai, China) was used to stain the cells on day 6 after osteogenesis induction. In brief, the cells were initially fixed in 4 % paraformaldehyde, rinsed with PBS, stained with BCIP/NBT reagent and then rinsed again for observation.

Quantitative real-time polymerase chain reaction

The MC3T3-E1 cells were treated with 10 μg/mL MSN@PEI-KALA, MSN_miR-NC@PEI-KALA, and MSN_miR-199a@PEI-KALA. To investigate the efficiency of MSN_miR-199a@PEI-KALA as delivery system, miR-199a expression level of MC3T3-E1 after transfection for 12 h were detected by Quantitative Real-Time Polymerase Chain Reaction (qRT-PCR). 7 days after osteogenic induction, qRT-PCR was used to measure the mRNA expression of markers of osteogenic differentiation, such as ALP, runt-related transcription factor 2 (RUNX2), and osteopontin (OPN). The CFX96 Real-Time PCR machine (BIO-RAD, Hercules, CA, USA) was used to perform qRT-PCR after the cDNA was reverse transcribed. β-actin served as the internal control for the evaluation of mRNA expression, and U6 was utilized as an internal standard to identify miRNA. The $2^{\Delta\Delta CT}$ method was utilized to determine the relative expression of each reaction, which was carried out in triplicate (Table 1).

Statistical analysis

The mean values derived from at least three technical replicates are used to present experimental values. The standard error of the mean is displayed with the mean values. Prism 9.5.0 (GraphPad Software, San Diego, CA, USA) was used to analyze the data. One-way or two-way analysis of variance was used to compare the groups with each other. $P < 0.05$ was regarded as the threshold for statistical significance.

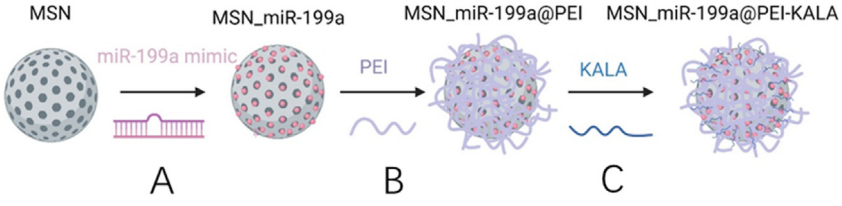

Figure 1 Flowchart for the construction of MSN_miR-199a@PEI-KALA nanoparticles. A: MiR-199a mimics are encapsulated within MSN mesopores; B: PEI coating MSN_miR-199a; C: Attaching KALA peptides to MSN_miR-199a@PEI's surface. Created with BioRender.com.

Table 1 Primer sequences used for qRT-PCR analysis.

Gene	Forward	Reverse
ALP	5′-GTTGTTGTGAGCGTAATCTACC-3′	5′-TCATTCCCACGTTTTCACATTC-3′
OPN	5′-AAACACACAGACTTGAGCATTC-3′	5′-TTAGGGTCTAGGACTAGCTTGT-3′
Runx2	5′-TGCTATTGCCCAAGATTTGC-3′	5′-GAGGGGGAAATGCCAAATAA-3′
β-actin	5′-TATGCTCTCCCTCACGCCATCC-3′	5′-GTCACGCACGATTTCCCTCTCAG-3′

Results

Characterization of nanoparticles

The morphology of the MSNs, MSN@PEI-KALA, MSN_miR-NC@PEI-KALA and MSN_miR-199a@PEI-KALA were observed by TEM (Fig. 2). Figs. 3 and 4 display the zeta potential and size of the four different types of particles as determined by the DLS experiment. After coated with PEI, the particle's zeta potential changed from negative to positive (Fig. 3A–D), proving that PEI was effectively modified onto MSN. Compared to MSN@PEI-KALA, both MSN_miR-NC@PEI-KALA and MSN_miR-199a@PEI-KALA possess a smaller size and a higher positive potential, which is more favorable for the nanoparticles to penetrate the cell membrane.

Cell viability

In Fig. 5, MC3T3-E1 was cultured with MSN@PEI-KALA, MSN_miR-NC@PEI-KALA, and MSN_miR-199a@PEI-KALA at different particle concentrations for 48 h in order to test the viability of the cells. The untreated cells were designated as the control group. MSN_miR-199a@PEI-KALA showed the lowest cytotoxicity to MC3T3-E1 at a dose of 10 μg/mL compared with the control.

Localization and uptake of miRNA

In Fig. 6, nuclei are depicted by blue staining, while intracellular lysosomes are depicted by red fluorescence, miR-199a molecules are represented by green fluorescence and exhibit biodistribution in a dot-like granular pattern that overlaps with the red staining. Red and green fluorescence overlaps, suggesting that the cell has internalized MSN_miR-199a@PEI-KALA into the lysosome.

Alkaline phosphatase staining

In Fig. 7, cells were treated with MSN_miR-199a@PEI-KALA and results showed higher ALP staining intensity than other groups after 6 days of osteogenic induction. According to staining results, the introduction of MSN_miR-199a@PEI-KALA into MC3T3-E1 cells facilitated early osteoblast differentiation.

Quantitative real-time polymerase chain reaction analysis of transfection efficiency and osteogenic gene expression

Compared to the other groups, MSN_miR-199a@PEI-KALA had a considerably increased miR-199a level. However, there was no apparent distinction between the control and MSN@PEI-KALA and MSN_miR-NC@PEI-KALA-treated cells (Fig. 8). The qPCR results showed that a high transfection efficiency could be achieved with a low quantity of 10 μg/mL of MSN_miR-199a@PEI-KALA, thus promoting the osteogenic differentiation of MC3T3-E1.

After 7 days of osteogenic induction, MC3T3-E1 treated with MSN_miR-199a@PEI-KALA exhibited the greatest levels of ALP, OPN, and Runx2 (Fig. 9). The levels of OPN expression in the other three groups did not differ significantly. ALP levels were considerably greater in cells treated with MSN_miR-NC@PEI-KALA, whereas Runx2 levels were considerably higher in cells treated with MSN_PEI-KALA. The reason for this needs to be investigated further.

Discussion

miRNAs exert a vital role in upholding biological homeostasis by regulating essential processes such as cell proliferation, differentiation, survival, apoptosis, and epithelial-

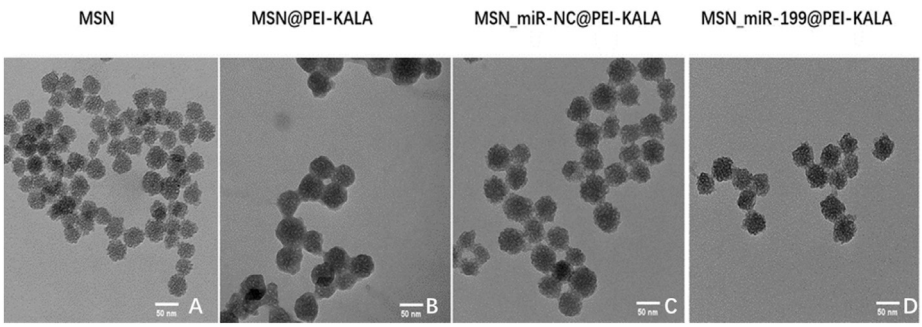

Figure 2 TEM images of the four nanoparticles. A: MSNs; B: MSN@PEI-KALA; C: MSN_ miR-NC@PEI-KALA; D: MSN_miR-199a@PEI-KALA. The scale bar in each micrograph represents a distance of 50 nm.

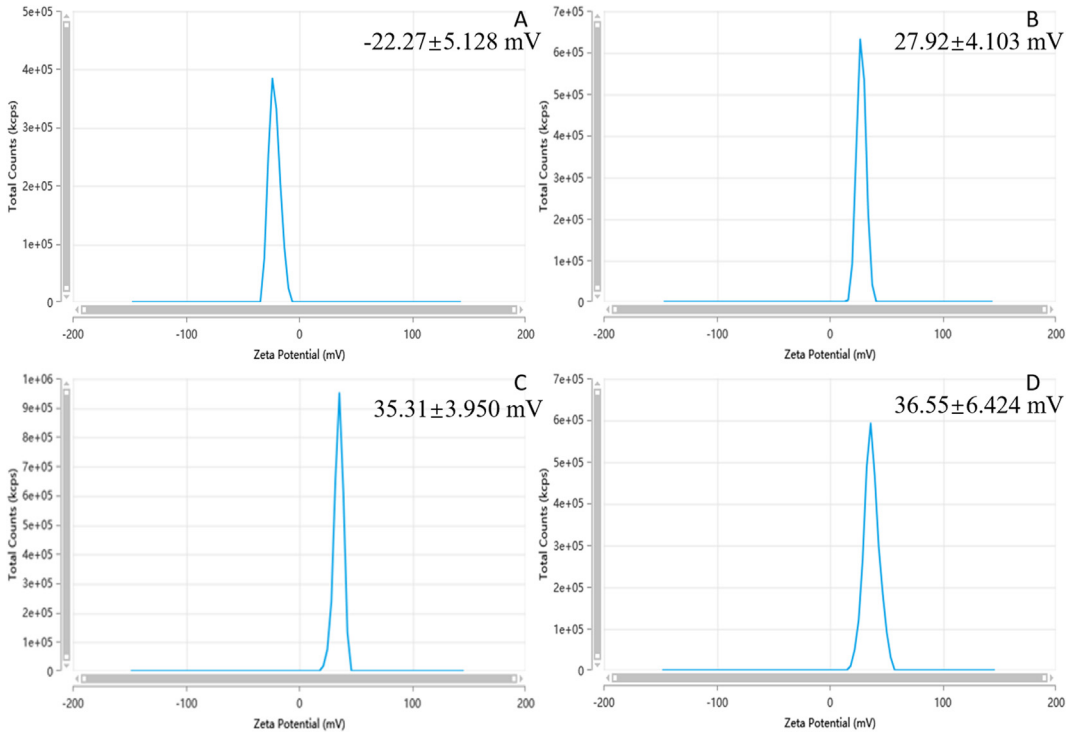

Figure 3 Zeta potential distributions. A: MSNs; B: MSN@PEI-KALA; C: MSN_miR-NC@PEI-KALA; D: MSN_miR-199a@PEI-KALA.

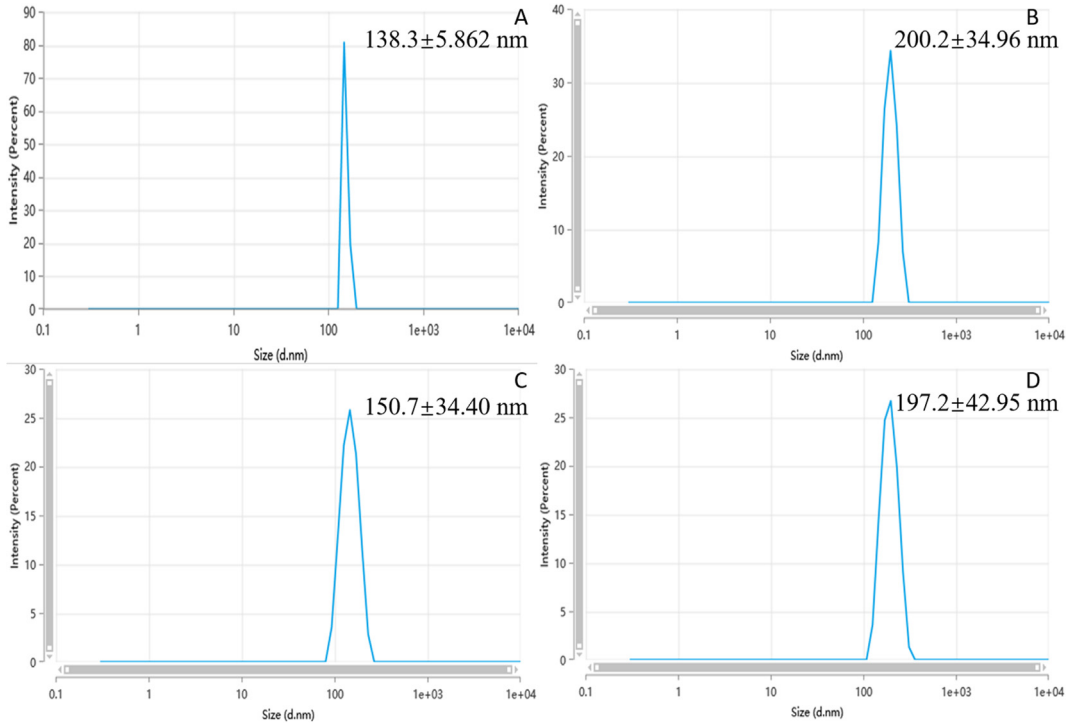

Figure 4 Particle size distributions. A: MSNs; B: MSN@PEI-KALA; C: MSN_miR-NC@PEI-KALA; D: MSN_miR-199a@PEI-KALA.

to-mesenchymal transition.[26] Numerous bone illnesses, such as osteopetrosis, osteogenesis imperfecta, and bone cancers, have been linked to dysregulation of miRNAs.[27] Extensive research has explored the clinical potential of miRNAs in bone-related diseases and regenerative medicine. In addition to controlling signaling pathways and transcription factors involved in osteogenesis, miRNAs are essential for regulating the differentiation of osteoblasts, osteoclasts, and chondrocytes.[28,29] Regenerative medicine therapies based on miRNAs are also gaining more

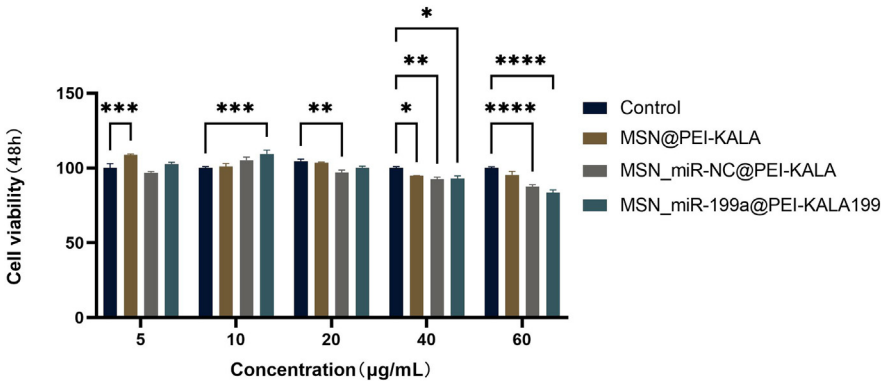

Figure 5 Cell viability of particles with CCK-8 Assay after 48 h incubation period at different particle concentrations (When compared to the control, $^{*}P < 0.05$, $^{**}P < 0.01$, $^{***}P < 0.001$, $^{****}P < 0.0001$).

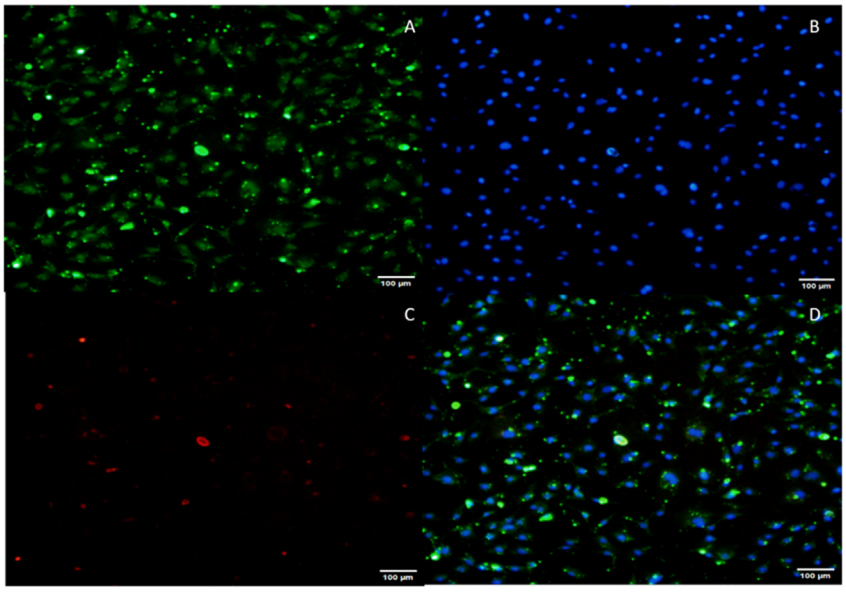

Figure 6 Fluorescent stained images of MC3T3-E1 cells incubated with FAM-labelled MSN_miR-199a@PEI-KALA after 6 h. A: miR-199a; B: Nuclei; C: Lysosome; D: Merged. The scale bar in each micrograph represents a distance of 100 μm.

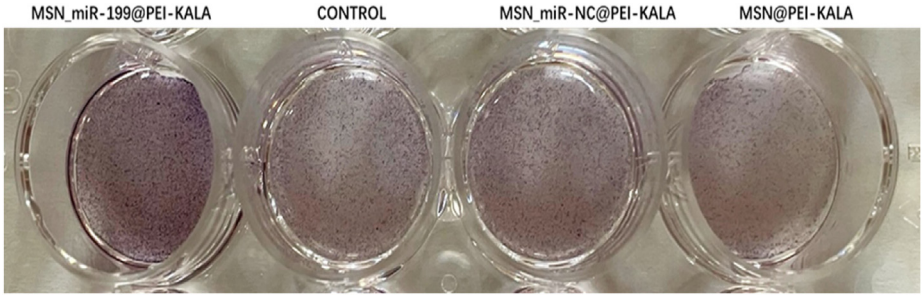

Figure 7 ALP staining of MC3T3-E1 incubated with various particles following 6 days of osteogenic induction.

attention.[30,31] However, delivering miRNA encounters various challenges as a result of drawbacks like susceptibility to degradation, significant negative charge, and barriers in traversing cellular membranes.

The process of bone regeneration is a key part of dental implant treatment.[32] Accelerated bone healing is an important key to successful implant therapy.[33] Although there are many reports on bone grafting surgical techniques and materials, there are few methods to promote endogenous bone healing capacity. In our previous article, we analyzed miRNAs encapsulated in osteoblast-derived exosomes and investigated miRNAs involved in osteoblast

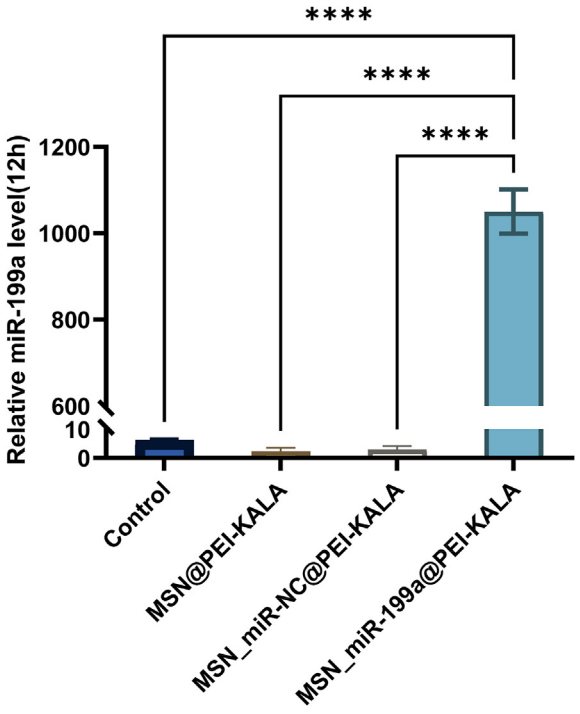

Figure 8 qRT-PCR evaluation of miR-199a level at 12 h after transfection (****$P < 0.0001$ compared with the control).

differentiation of periosteal cells. In vitro, exosomes from osteoblasts promote the osteogenic differentiation of periosteum-derived cells (PDCs). Additionally, co-culturing with osteoblasts promoted the expression of exo-miRs sets that could be relevant to apoptosis of muscle/fibrous cells.[34] Among the miRNA sets previously shown to induce osteoblastic differentiation of PDCs from our results, we focused on miR-199. Based on the findings of the prior work, by targeting TET2, miR-199a-5p could enhance osteoblast development and block OVX-induced osteoporosis.[35] Apical periodontitis patients had reduced expression of miR-199a-5p in their periapical tissues, and miR-199a-5p mimics significantly increased the cell proliferation and osteogenesis differentiation of human stem cells from apical papilla, while miR-199a-5p antagomir significantly reduced the osteogenesis.[36] This study investigated the potential of MSN as carriers to deliver miR-199a-5p in bone regeneration therapy. This miR-199a-5p delivery system was designed by combining three crucial factors: (1) MSN has good biocompatibility, but cannot be directly loaded with nucleic acids due to its negative charge in aqueous solution; (2) PEI served as the ligand to coat the surface, which helps in enhancing cell adhesion and aggregation. However, the effect of PEI is bio-toxic at high concentrations;[37] (3) The KALA peptide not only improves particle agglomeration but also reduces the toxicity of PEI.[38]

The findings from the CCK-8 assay indicate that as concentrations increased, there wasn't a notable decline in cell viability within the MSN@PEI-KALA group when contrasted with both MSN_miR-NC@PEI-KALA and MSN_miR-199a@PEI-KALA, presumably because the delivery complex was not significantly cytotoxic.

The qPCR results showed that, despite a low concentration of 10 μg/mL of MSN_miR-199a@PEI-KALA, a high transfection efficiency could be achieved, thus promoting the osteogenic differentiation. Its effectiveness in inducing bone regeneration is strongly supported by the enhanced expression of the osteogenic markers ALP, OPN, and Runx2 with MSN_miR-199a@PEI-KALA following osteogenic induction. Therefore, this nanocarrier miR-199a-5p is promising as a potential strategy to promote endogenous bone healing.

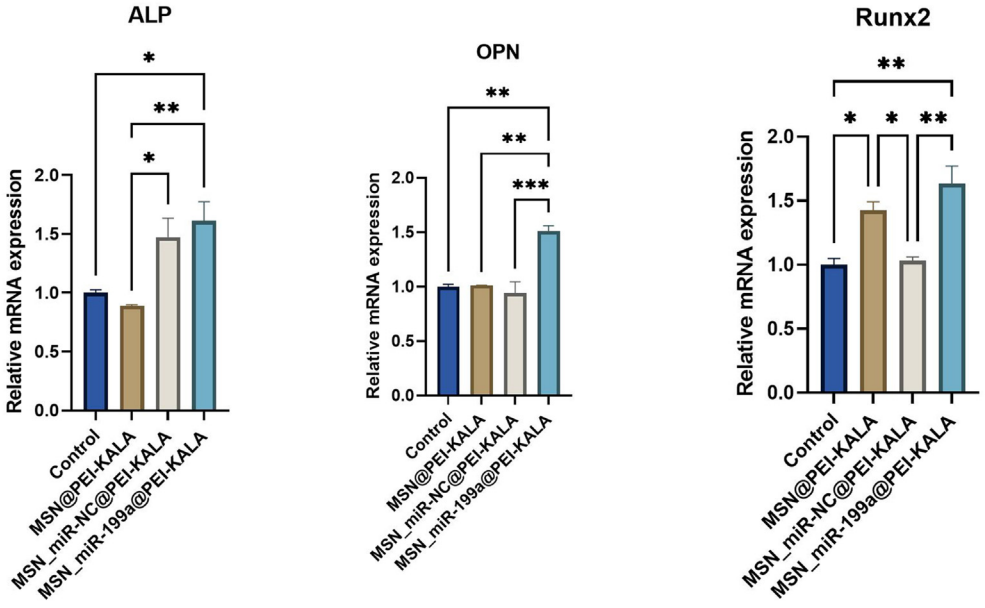

Figure 9 Relative mRNA expression of genes associated with osteogenesis, ALP, OPN, and Runx2, in MC3T3-E1 incubated with various particles following a 7-day period of osteogenic induction (*$P < 0.05$, **$P < 0.01$, ***$P < 0.001$, compared with the control).

However, further molecular mechanism research and animal experiments are needed to fully evaluate the long-term effects, scalability, safety and clinical translation of these delivery systems. Nonetheless, the findings presented herein provide a solid foundation for advancing miR-199a-based treatment methods for bone defects and related diseases in the future. Targeted delivery of miR-199a can stimulate bone-forming cells, which will speed up the repairing procedure. It may be feasible to treat osteoporosis and enhance the integration of implants into natural bone structures by using nanocarriers to deliver miR-199a.

Declaration of competing interest

The authors have no conflicts of interest relevant to this article.

Acknowledgements

This research was supported by the Japanese Society for the Promotion of Sciences (Grant no. 23K19738) and PhD program of Tokyo Medical and Dental University.

The authors sincerely thank Dr. Katarzyna Inoue, Department of Biochemistry, and Dr. Kei Sakamoto, Department of Oral Pathology, Dr. Yukihiko Tamura, Department of Cariology and Operative Dentistry, Tokyo Medical and Dental University for the borderless education of TMDU PhD program, Prof. Wei Wang, Department of Parasitology, Anhui Medical University, School of Basic Medical Science for the technical advice.

References

1. Sreenivasalu PKP, Dora CP, Swami R, et al. Nanomaterials in dentistry: current applications and future scope. *Nanomaterials (Basel)* 2022;12:1676.
2. Abiodun-Solanke I, Ajayi D, Arigbede A. Nanotechnology and its application in dentistry. *Ann Med Health Sci Res* 2014;4:S171—7.
3. Abou Neel EA, Bozec L, Perez RA, Kim HW, Knowles JC. Nanotechnology in dentistry: prevention, diagnosis, and therapy. *Int J Nanomed* 2015;10:6371—94.
4. Jandt KD, Watts DC. Nanotechnology in dentistry: present and future perspectives on dental nanomaterials. *Dent Mater* 2020;36:1365—78.
5. Paris JL, Vallet-Regi M. Mesoporous silica nanoparticles for co-delivery of drugs and nucleic acids in oncology: a review. *Pharmaceutics* 2020;12:526.
6. Jat SK, Bhattacharya J, Sharma MK. Nanomaterial based gene delivery: a promising method for plant genome engineering. *J Mater Chem B* 2020;8:4165—75.
7. Riley MK, Vermerris W. Recent advances in nanomaterials for gene delivery-a review. *Nanomaterials (Basel)* 2017;7:94.
8. Xu C, Cao Y, Lei C, et al. Polymer—mesoporous silica nanoparticle core—shell nanofibers as a dual-drug-delivery system for guided tissue regeneration. *ACS Appl Nano Mater* 2020;3:1457—67.
9. Frickenstein AN, Hagood JM, Britten CN, et al. Mesoporous silica nanoparticles: properties and strategies for enhancing clinical effect. *Pharmaceutics* 2021;13:570.
10. Manzano M, Vallet-Regí M. New developments in ordered mesoporous materials for drug delivery. *J Mater Chem* 2010;20:5593—604.
11. Manzano M, Colilla M, Vallet-Regi M. Drug delivery from ordered mesoporous matrices. *Expet Opin Drug Deliv* 2009;6:1383—400.
12. Xu C, Lei C, Yu C. Mesoporous silica nanoparticles for protein protection and delivery. *Front Chem* 2019;7:290.
13. Tang F, Li L, Chen D. Mesoporous silica nanoparticles: synthesis, biocompatibility and drug delivery. *Adv Mater* 2012;24:1504—34.
14. Li X, Chen Y, Wang M, Ma Y, Xia W, Gu H. A mesoporous silica nanoparticle-pei-fusogenic peptide system for sirna delivery in cancer therapy. *Biomaterials* 2013;34:1391—401.
15. Xue L, Yan Y, Kos P, Chen X, Siegwart DJ. Pei fluorination reduces toxicity and promotes liver-targeted sirna delivery. *Drug Deliv Transl Res* 2021;11:255—60.
16. Wyman TB, Nicol F, Zelphati O, Scaria PV, Plank C, Szoka Jr FC. Design, synthesis, and characterization of a cationic peptide that binds to nucleic acids and permeabilizes bilayers. *Biochemistry* 1997;36:3008—17.
17. Yan C, Shi W, Gu J, Lee RJ, Zhang Y. Design of a novel nucleus-targeted nls-kala-sa nanocarrier to delivery poorly water-soluble anti-tumor drug for lung cancer treatment. *J Pharmaceut Sci* 2021;110:2432—41.
18. Yamada Y, Ishikawa T, Harashima H. Validation of the use of an artificial mitochondrial reporter DNA vector containing a cytomegalovirus promoter for mitochondrial transgene expression. *Biomaterials* 2017;136:56—66.
19. Miura N, Akita H, Tateshita N, Nakamura T, Harashima H. Modifying antigen-encapsulating liposomes with kala facilitates mhc class i antigen presentation and enhances anti-tumor effects. *Mol Ther* 2017;25:1003—13.
20. Hosseinpour S, Dai H, Walsh LJ, Xu C. Mesoporous core-cone silica nanoparticles can deliver mirna-26a to macrophages to exert immunomodulatory effects on osteogenesis in vitro. *Nanomaterials (Basel)* 2023;13:1755.
21. Yan J, Lu X, Zhu X, et al. Effects of mir-26a on osteogenic differentiation of bone marrow mesenchymal stem cells by a mesoporous silica nanoparticle - pei - peptide system. *Int J Nanomed* 2020;15:497—511.
22. Chen X, Gu S, Chen BF, et al. Nanoparticle delivery of stable mir-199a-5p agomir improves the osteogenesis of human mesenchymal stem cells via the hif1a pathway. *Biomaterials* 2015;53:239—50.
23. Guo K, Zhang D, Wu H, Zhu Q, Yang C, Zhu J. Mirna-199a-5p positively regulated rankl-induced osteoclast differentiation by target mafb protein. *J Cell Biochem* 2019;120:7024—31.
24. Kim BK, Yoo HI, Kim I, Park J, Kim Yoon S. Fzd6 expression is negatively regulated by mir-199a-5p in human colorectal cancer. *BMB Rep* 2015;48:360—6.
25. Guo W, Qiu Z, Wang Z, et al. Mir-199a-5p is negatively associated with malignancies and regulates glycolysis and lactate production by targeting hexokinase 2 in liver cancer. *Hepatology* 2015;62:1132—44.
26. Seeliger C, Balmayor ER, van Griensven M. Mirnas related to skeletal diseases. *Stem Cell Dev* 2016;25:1261—81.
27. Gennari L, Bianciardi S, Merlotti D. Micrornas in bone diseases. *Osteoporos Int* 2017;28:1191—213.
28. Papaioannou G. Mirnas in bone development. *Curr Genom* 2015;16:427—34.
29. Lian JB, Stein GS, van Wijnen AJ, et al. Microrna control of bone formation and homeostasis. *Nat Rev Endocrinol* 2012;8:212—27.
30. Gong T, Xie J, Liao J, Zhang T, Lin S, Lin Y. Nanomaterials and bone regeneration. *Bone Res* 2015;3:15029.
31. Frohlich LF. Micrornas at the interface between osteogenesis and angiogenesis as targets for bone regeneration. *Cells* 2019;8:121.
32. Dam VV, Trinh HA, Rokaya D, Trinh DH. Bone augmentation for implant placement: recent advances. *Int J Dent* 2022;2022:8900940.

33. Donos N, Akcali A, Padhye N, Sculean A, Calciolari E. Bone regeneration in implant dentistry: which are the factors affecting the clinical outcome? *Periodontol* 2000;2023:1—30.
34. Yokota K, Nakata H, Miura M, Kasugai S, Kuroda S. Effect of osteoblast/periosteal cell-derived exosomes on periosteal cells during osteogenic differentiation. *J Stomatol Soc Japan* 2021; 88:102—14.
35. Qi XB, Jia B, Wang W, et al. Role of mir-199a-5p in osteoblast differentiation by targeting tet2. *Gene* 2020;726:144193.
36. Hu J, Huang X, Zheng L, et al. Mir-199a-5p promotes osteogenic differentiation of human stem cells from apical papilla via targeting ifit2 in apical periodontitis. *Front Immunol* 2023;14: 1149339.
37. Liu S, Yue H, Ho SL, et al. Polyethylenimine-coated ultrasmall holmium oxide nanoparticles: synthesis, characterization, cytotoxicities, and water proton spin relaxivities. *Nanomaterials (Basel)* 2022;12.
38. Tateshita N, Miura N, Tanaka H, et al. Development of a lipoplex-type mrna carrier composed of an ionizable lipid with a vitamin e scaffold and the kala peptide for use as an ex vivo dendritic cell-based cancer vaccine. *J Contr Release* 2019;310: 36—46.